Energy Management of Airport Service Electric Vehicles to Match Renewable Generation through Rollout Approach

Renjie Wei
State Grid Laboratory of Grid Advanced Computing and Applications
State Grid Smart Grid Research Institute Co., Ltd
Beijing, China
wrj245478404@hotmail.com

Yishen Wang
State Grid Laboratory of Grid Advanced Computing and Applications
State Grid Smart Grid Research Institute Co., Ltd
Beijing, China
wangyishen07@163.com

Fei Zhou
State Grid Laboratory of Grid Advanced Computing and Applications
State Grid Smart Grid Research Institute Co., Ltd
Beijing, China
zhoufei@geiri.sgcc.com.cn

***Abstract*—Traditional diesel-based airport service vehicles are characterized by a heavy-duty, high-usage-frequency nature and a high carbon intensity per vehicle per hour. Transforming these vehicles into electric vehicles would reduce CO2 emissions and potentially save energy costs in the context of rising fuel prices, if a proper energy management of airport service electric vehicles (ASEVs) is performed. To perform such an energy management, this paper proposes a new customized rollout approach, as an optimal control method for a new ASEV dynamics model, which models the ASEV states, their transitions over time, and how control decisions affect them. The rollout approach yields an optimal control strategy for the ASEVs to transport luggage and to charge batteries, with the objective to minimize the operation cost, which incentivizes the charging of the ASEVs to match renewable generation. Case studies demonstrate that the rollout approach effectively overcomes the "curse of dimensionality" challenge. The rollout algorithm results in a total cost approximately 10% less than that of the underlying "greedy charging" heuristic, which charges a battery whenever its state of charge is not the maximum. The rollout algorithm is proven to be adaptive towards flight schedule changes at short notice.**

***Index Terms*-- airport service electric vehicle; electric vehicle; energy management; heuristic control; optimal control; rollout algorithm.**

I. INTRODUCTION

The transition to electric vehicles (EVs) is vital for fulfilling the target of reducing CO2 emissions by 80% by 2050 in the UK, relative to the 1990's level [1]. Much attention was devoted to electrifying tens of millions of consumer vehicles. Although they are vast in number, they have a relatively low carbon intensity in terms of emission per vehicle per hour, because an average consumer vehicle remains dormant in most hours of a day and it is of a light-duty nature. Unlike consumer vehicles, airport service vehicles are characterized by a heavy-duty, high-usage-frequency nature, a high carbon intensity per vehicle per hour, and a strong correlation with flight patterns. Transforming diesel-based airport service vehicle fleets into EVs would be one of the effective adoption to reduce CO2 emissions for this carbon-intensive industry. In this context, airport service electric vehicles (ASEVs) specifically refer to electric trailers that transport checked luggage between the sorting facility in the terminal and departure/arrival flights. The aim of this paper is to develop an optimal energy management strategy for the ASEVs in terms of battery charging and task assignment.

Existing research work focuses on consumer EVs and taxis at different locations, e.g. households, office buildings, highway service stations, etc. References [2], [3] focus on consumer EV charging at commercial buildings. A number of references consider domestic EVs as a part of home energy management systems [4], [5], [6], an energy hub [7] or a community energy system [8]. A number of references investigate the operation of electric vehicle parking lots [9], [10], including airport parking lots [11]. References [12], [13] both develop stochastic optimization models for the joint operation of EV fleets and renewable generation. Reference [14] develops a balanced charging strategy to satisfy both the EV

Submitted to the 23rd Power Systems Computation Conference (PSCC 2024).
This work was supported by State Grid Corporation of China Technical Funding under Grant 5700-202358705A-3-3-JC.

owners (saving costs) and the network operator (relieving loads). Reference [15] develops an optimization model to schedule airport ground operations, including aircraft and shuttle bus scheduling. Although that reference does not focus on EVs, it acknowledges the importance of the optimization of airport ground operations.

There are ASEV suppliers [17], [18], [19], but the optimal control of the ASEVs was an unanswered question. For an airport with tens of ASEVs, the dynamic system has a prohibitively large number of states (i.e. the "curse of dimensionality"), too large to derive an accurate optimal solution to the ASEV control problem. Therefore, two research questions arise from the optimal scheduling of ASEVs: 1) the modeling of the ASEVs as a distinctive dynamic system of a stochastic dynamic, hybrid nature; and 2) the derivation of an optimal control strategy for the dynamic system.

The optimal control of a dynamic system is related to stochastic dynamic programming [16] [20] in terms of their stochastic and dynamic nature. The rollout algorithm for dynamic programming [20], [21] can be borrowed but it needs to be adapted for the optimal control of ASEVs: the underlying heuristic control strategies need to be defined and uncertainties need to be properly modeled.

Thus, to better control the ASEV considering their characteristics, this paper proposed a dynamic programming approach based on rollout method, which would not only guide the EV charging, but also matching the PV generation to improve the energy efficiency. This paper makes the following original contributions:

1) This paper proposes a new ASEV dynamics model. The model involves: i) discrete dynamics, i.e. the changes of the ASEV discrete states to "work", "charge", or "idle" over time; ii) continuous dynamics, i.e. the changes of the battery state of charge (SoC) over time; and iii) a stochastic nature of the ground transport workload.

2) To perform an energy management of the ASEVs, this paper proposes a new customized rollout approach, as an optimal control method for the ASEV dynamics model. The approach controls the ASEVs to transport luggage and to charge batteries, with the objective to minimize the total operation cost. Two customized suboptimal heuristic control strategies are proposed as the base strategies for the rollout approach, which then iteratively improves the heuristic control strategies into an optimal control strategy. The rollout approach effectively overcomes the "curse of dimensionality" challenge.

The energy management of ASEVs through the rollout approach will bring a number of benefits: 1) it will save costs for the airport; 2) by matching the ASEV battery charging load curve with renewable generation, the control method encourages the ASEVs to consume locally generated renewable energy, reduces CO_2 emissions, and makes the charging load curve friendly to the grid.

The rest of this paper is organized as follows: Section II presents the ASEV dynamics model; Section III presents the optimal control method for the ASEV dynamics model; Section IV performs case studies; and Section V concludes the paper.

II. Problem Formulation: ASEV Dynamics Model

The ASEV uncertainties are divided into two different parts: the uncertainties of the ground transport workloads and the uncertainties of the flights. For the uncertain ground transport workloads, the proposed model adopted an appropriate model which is explained in Section II-A. For the uncertainties of the flights, including the flights delaying or cancelling, a Guassian noise is added to the model to reflect the delaying time of each flight.

A. Modeling of Uncertain Ground Transport Workload

Before presenting the ASEV dynamics model, the ground transport workload model is presented. Suppose the *j*th flight is awaiting ground transport service at time *t* (called flight *j* at time *t*), because it has landed or is ready to depart. The time required for an ASEV to serve this flight is stochastic because: 1) although the airline company knows the number of passengers and luggage weight for the flight in question, the information may not be shared with the airport. 2) Even if the information were made available to the airport, there is a random noise in the time required to service the flight. Denote the time required for an ASEV to serve flight *j* at time *t* as $\widetilde{w}_{jt}$, which follows a truncated normal distribution ψ [22].

$$\psi\left(\mu,\sigma,a,b,\widetilde{w}_{jt}\right) = \begin{cases} 0 & \text{if } \widetilde{w}_{jt} \le a \\ \dfrac{\emptyset\left(\mu,\sigma^2;\ \widetilde{w}_{jt}\right)}{\Phi(\mu,\sigma^2;b)-\Phi(\mu,\sigma^2;a)} & \text{if } b \le \widetilde{w}_{jt} \le a \\ 0 & \text{if } \widetilde{w}_{jt} \ge b \end{cases} \quad (1)$$

where μ and σ are the mean and deviation of the "parent" normal distribution, respectively. a and b are the upper and lower bounds, respectively. $\emptyset(\mu,\sigma^2;\ x)$ and $\Phi(\mu,\sigma^2;x)$ are the probability density function and cumulative distribution function, respectively, of the "parent" normal distribution with mean μ and deviation σ. The truncated normal distribution model is justified because: 1) a normal distribution is a default choice when there is no detailed knowledge to support alternative complicated probability distributions; and 2) $\widetilde{w}_{jt}$ is bounded in reality.

Suppose that the 24 hours of a day are discretised into 144 stages, starting from Stage 0 to Stage 143 at an interval of 10 minutes. Let w_{jt} denote the discrete number of stages (essentially the amount of time) required for an ASEV to serve the *j*th flight that is awaiting service at Stage *t*. Therefore, w_{jt} is a random discrete variable.

Now the continuous random variable $\widetilde{w}_{jt}$ is discretized into w_{jt}: first, divide the time range of $[b,a]$ into m stages at an interval of $\Delta t = 5$ minutes (assuming that the length of $[b,a]$ is $m\Delta t$). These m stages are represented by m integers from $b/\Delta t$ to $a/\Delta t - 1$, therefore, $w_{jt} \in [b/\Delta t\ , a/\Delta t - 1]$ and w_{jt}

is an integer. Secondly, the probability of w_{jt} taking value k out of the m values is given by

$$\text{Prob}(w_{jt} = k) = \Phi(\mu, \sigma^2; \rho_u) - \Phi(\mu, \sigma^2; \rho_l) \quad (2)$$

where Φ is the cumulative distribution function as defined in (1). ρ_u and ρ_l are the upper and lower bounds of $\widetilde{w}_{jt}$ within Stage k, respectively. w_{jt} is the discretized random workload, as explained above. For example, $w_{jt} \in \{3, 4, 5, 6\}$, meaning that the ground transport for the *j*th flight at Stage t requires 15 minutes ($w_{jt} = 3$ stages) to 30 minutes ($w_{jt} = 6$ stages) to complete. The probability of w_{jt} taking each discrete value is derived in (2). w_{jt} is a critical input for the ASEV dynamics model introduced in Section II –B.

B. ASEV dynamics model

In this chapter, an ASEV dynamics model is presented, which models the control decisions, the ASEV states and their transitions over time. The model considers the uncertain ground transport workload as modelled in Section II-A.

At any Stage *t* (time is discretised into stages), the ASEV fleet state S_t consists of the states of all individual ASEVs. S_{it} denotes the state of an *i*th ASEV at Stage *t*, given by:

$$S_{it} = [q_{it}, SoC_{it}, f_{Rit}] \quad (3)$$

where q_{it} is a discrete state: $q_{it} = 1$ means that the *i*th ASEV is charging at Stage *t*; $q_{it} = 0$ means that it is idling; $q_{it} < 0$ means that it is working (in this paper, "working" means undertaking ground transport) and it will take $|q_{it}|$ stages to complete the work. SoC_{it}, a continuous state, is the state of charge (SoC) of the ith ASEV's battery at Stage *t*. f_{Rit} denotes the battery cycles to failure for the *i*th ASEV at Stage *t*.

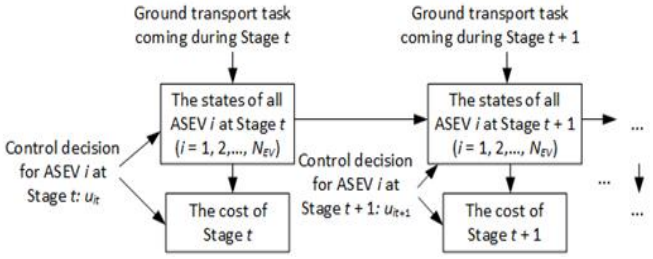

Figure 1. Overview of the ASEV dynamics model.

According to Fig. 1, the optimal control is performed online, i.e. the control decision for each Stage *t* is made when the state S_{it} at Stage *t* becomes known.

The energy cost for the *i*th ASEV at Stage *t* is given by:

$$C_{it} = \begin{cases} C_R \cdot max\{q_{it}, 0\} \cdot E_c & \text{if } max\{q_{it}, 0\} \cdot E_c \le E_{Rt} \\ C_R E_{Rt} + C_{Gt}(max\{q_{it}, 0\} \cdot E_c - E_{Rt}) & \text{otherwise} \end{cases} \quad (4)$$

where C_R denotes the energy price per kWh from renewable generation. E_c denotes the energy consumption (some of the energy is charged to the battery and the rest is lost) during each stage. E_c is a constant given the assumption of the constant battery charging power. C_{Gt} denotes the price per kWh of the grid-supplied energy at Stage *t*. E_{Rt} denotes the available energy generated by renewable generation at Stage *t*. q_{it} is given in (3). The "max" term in (4) ensures that the energy cost is incurred only when the ASEV is charging. Equation (4) is based on the principle that the ASEV fleet gives priority to consuming the cheap energy directly purchased from renewable generation over consuming the grid-supplied energy. For the E_{Rt}, it is assumed to be accurately predicted by a combination of historical data and prediction algorithms and for each time stage, it is known to the airport control system.

The battery degradation cost for the *i*th ASEV at Stage *t* is given by

$$B_{it} = f(SoC_{it}, E_w, f_{Rit}) \quad \text{if } q_{it} < 0 \quad (5)$$

where q_{it}, SoC_{it} and f_{Rit} are given in (3). E_w is the energy discharged during Stage *t*. Function *f* is the linear function for battery degradation cost during its normal charging-discharging cycles, with its coefficient derived from [23]. It is the function of the SoC, energy discharged during Stage *t*, and the cycles to failure. If the battery is over-charged or deep discharged, some parameters in this function will be changed and the degradation cost increases more with the same energy discharged.

The total cost (including energy and battery degradation costs) for all ASEVs at Stage *t* is given by:

$$g_t = \sum_{i=1}^{N_{EV}} (C_{it} + B_{it}) \quad t = 0,1,2 \dots, N-1 \quad (6)$$

where C_{it} and B_{it} are given in (4) and (5), respectively. N_{EV} is the total number of ASEVs.

Ideally, all ASEV batteries, except for those which is under work state or just finishing work, should be charged to full at the end of the day to prepare the ASEVs for ground transport the next day. If any battery is not charged to full at the last stage of the day (Stage *N*), this incurs a terminal stage cost. Also, if a flight needs the ASEV but there is no ASEV available, a punishment for the delay is added. In this paper, it is included in the terminal stage cost because it is calculated at the end of each day. The terminal stage cost is given by:

$$g_N = \sum_{i=1}^{N_{EV}} C_{GN} B(SoC_{max} - SoC_{iN}) + \sum_{i=1}^{N_{delay}} T_{delayi} C_{punishment} \quad (7)$$

where C_{GN} denotes the price per kWh of the grid-supplied energy at Stage *N*. *B* denotes the battery energy capacity. SoC_{max} is the upper bound of the SoC. N_{EV} is the total number of ASEVs. SoC_{iN} denotes the SoC of the *i*th ASEV at Stage *N*.

N_{delay} is the total number of times of ASEV delay on the day and $T_{delay,i}$ is the duration of the *i*th ASEV delay. $C_{punishment}$ denotes the punishment cost per time slot.

The objective of the ASEV optimal control is to minimize the summation of g_t over all stages of the day.

$$\text{Min } J = g_N + \sum_{t=0}^{N-1} g_t \tag{8}$$

where g_t and g_N are given in (6) and (7), respectively.

When the SoC of the *i*th ASEV battery reaches either the upper bound or the lower bound, there are two state constraints:

Case 1: an ASEV *i* is prevented from switching to work because of a low SoC.

$$\text{If } q_{it} \geq 0 \text{ and } SoC_{it} \leq SoC_{min}, \text{ then } q_{it+1} = u_{it} \geq 0 \tag{9}$$

where q_{it}, q_{it+1}, and SoC_{it} are defined in (3). SoC_{min} denotes the lower bound of the SoC. u_{it} is the control decision for ASEV *i* at Stage *t*: $u_{it} = 1$ means "to charge battery"; $u_{it} = 0$ means "to idle"; and $u_{it} = -1$ means "to work (i.e. undertake ground transport)".

Case 2: an ASEV *i* is prevented from battery charging because its SoC has reached the upper bound.

$$\text{If } q_{it} \geq 0 \text{ and } SoC_{it} = SoC_{max}, \text{ then } q_{it+1} = u_{it} \neq 1 \tag{10}$$

where q_{it}, q_{it+1}, and SoC_{it} are defined in (3). SoC_{max} is defined in (7); u_{it} is defined in (9).

When the SoC of the *i*th ASEV battery is above the lower bound and the ASEV is not currently working, a control-based state transition can occur. This is further divided into two cases:

Case 1: the ASEV *i* is controlled to work.

$$\text{If } SoC_{min} < SoC_{it} \text{ and } q_{it} \geq 0 \text{ and } u_{it} = -1, \text{ then } q_{it+1} = -w_{jt} \tag{11}$$

where SoC_{min} is defined in (9). q_{it}, q_{it+1}, and SoC_{it} are defined in (3). u_{it} is defined in (9). w_jt denotes the number of stages (the amount of time) required for an ASEV to serve the *j*th flight that is awaiting service at Stage *t*, as explained in Section II-A.

When a flight *j* is awaiting ground transport service at Stage *t*, it should be served as soon as there is at least one free ASEV.

$$\text{If } w_{jt} > 0 \text{ and } \exists i: q_{it} \geq 0 \text{ and } SoC_{it} > SoC_{min} + E_{wf}, \text{ then } \exists i: q_{it+1} = -w_{jt} \text{ and } u_{it} = -1 \tag{12}$$

where E_{wf} denotes the energy required for serving this flight and the other variables are defined the same as in (11).

If a flight *j* is awaiting service at Stage *t* but because no ASEV is available, the service for flight *j* is delayed to Stage *t* + 1. This translates to:

$$\text{if } w_{jt} > 0 \text{ and } \forall i: q_{it} < 0, \text{ then } w_{jt+1} = w_{jt} \text{ and } d_j \leftarrow d_j + 1 \quad t = 0,1,2 \ldots, N-1 \tag{13}$$

where w_{jt} is defined in Section II-A. q_{it} is defined in (3). d_j denotes the stages of delay. It is initialized to zero.

A hard constraint exists that the stages of service delay for any flight should be no more than a threshold.

$$d_j \leq d_{thre} \tag{14}$$

where d_{thre} is the threshold of delay; d_j is defined in (13).

Case 2: the ASEV *i* is controlled to idle or charge.

$$\text{If } SoC_{it} < SoC_{max} \text{ and } q_{it} \geq 0 \text{ and } u_{it} \geq 0, \text{ then } q_{it+1} = u_{it} \tag{15}$$

where SoC_{max} is defined in (7). q_{it}, q_{it+1}, and SoC_{it} are defined in (3). u_{it} is defined in (9).

When the *i*th ASEV is working, its work cannot be interrupted by any control decision. The ASEV will naturally complete the work. This is expressed as

$$\text{If } q_{it} \leq -2, \text{ then } q_{it+1} = q_{it} + 1 \text{ and } u_{it} = -1 \tag{16}$$

$$\text{If } q_{it} = -1, \text{ then } q_{it+1} = 0 \text{ and } u_{it} = 0 \tag{17}$$

where all variables are defined the same as in (12).

Fig. 2 presents a state transition graph describing the relation among q_{it}, w_{jt}, and u_{it}.

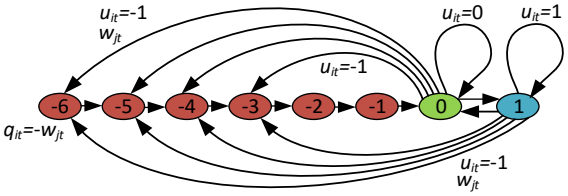

w_{jt} is a random discrete variable describing the number of stages required to serve flight *j*. In this example, w_{jt} belongs to the set {3, 4, 5, 6}, meaning that the ground transport requires at least 15 minutes (3 stages) and at most 30 minutes (6 stages) to complete.

Figure 2. State transition graph for the ith ASEV.

In Fig. 2, each circle represents a state of the *i*th ASEV. The value in each circle is q_{it}, i.e. the discrete state of the *i*th ASEV at Stage *t*. Red circles mean that the *i*th ASEV is working. The green and blue circles mean that the *i*th ASEV is idling and charging, respectively. As mentioned above, work cannot be interrupted. Therefore, in Fig. 2, the state transits naturally from -6 to 0 over time, as described by (16) and (17).

For any ASEV *i* at stage *t*, the continuous dynamics of its battery SoC depends on its control decision u_{it}.

$$SoC_{it+1} = \begin{cases} SoC_{it} - E_w & \text{if } u_{it} = -1 \\ SoC_{it} + min\{\gamma E_c, SoC_{max} - SoC_{it}\} & \text{if } u_{it} = 1 \\ SoC_{it} & \text{if } u_{it} = 0 \end{cases} \quad (18)$$

where SoC_{it} and SoC_{it+1} are defined in (3). Differently, in (18), the unit of SoC_{it} and SoC_{it+1} is kWh. u_{it} is defined in (9). E_w is defined in (5). E_c is the energy consumption during each stage, as defined in (4). γ is the efficiency of the battery. γE_c is therefore the energy charged to the battery during each stage.

With the ASEV dynamics model established, the next step is to determine a sequence of control variables u_{it} (defined in (9)) for all *i* (all ASEVs) and for all *t* (all stages of a day), with the objective to minimize the total operation cost (defined in (8)).

III. OPTIMAL CONTROL OF THE ASEV DYNAMICS MODEL

Based on the ASEV dynamics model detailed in the last chapter, a rollout approach is presented as an optimal control method to determine a sequence of control variables u_{it} for each ASEV at each stage *t*.

At each stage *t*, the optimal cost-to-go function J_t is defined as the minimum total cost from Stage *t* to Stage $N-1$ (the last stage of the day) plus the terminal stage cost g_N (as given by (7)). Because the prohibitively large number of states in the ASEV dynamics model cause a combinatorial explosion, it is impossible to calculate the accurate cost-to-go function J_t, thus being impossible to develop an accurate optimal control strategy for the ASEV dynamics model. A customized rollout approach is developed to yield an optimal control strategy through approximations. It consists of the following steps:

Two customized suboptimal heuristic control strategies are developed to approximate the cost-to-go function J_m as $\tilde{J}_m$, given the starting state S_m (the ASEV fleet state at Stage *m*). The two heuristics are elaborated as follows:

Heuristic i): the "renewable matching" heuristic. At each Stage *t* from Stage m to the last stage of the day, control the ASEVs to charge only when is available renewable energy as dictated by the renewable generation profile. When a flight is awaiting ground transport service, always assign the available ASEV with the greatest SoC to take the work.

Heuristic ii): the "greedy charging" heuristic. Given the starting state S_m at Stage *m*, control the ASEVs to charge as early as possible until the maximum SoC is reached. When a flight is awaiting ground transport service, always let the available ASEV with the greatest SoC take the work.

Heuristic i) is not always feasible because, when renewable energy is seriously deficient throughout the day, the ASEV batteries all have too low SoC values to undertake the "peak" workload of ground transport. If heuristic i) is not feasible from Stage *t*, then heuristic ii) is selected. If both heuristics are feasible from Stage *t*, the better one (the one that leads to a lower $\tilde{J}_t$) of the two heuristics is selected. The approximate cost-to-go $\tilde{J}_t$ for the selected heuristic is recorded for use in Step 2).

Given S_t (the ASEV fleet state at Stage *t*) which consists of S_{it} for all ASEVs *i*, the rollout approach generates the set of all possible S_{t+1} by enumerating all feasible control decisions u_{it} (defined in (9)) for Stage *t*, considering the workload w_{jt} (defined in (11)). The approach then selects the "best" S_{t+1} that produces the minimum approximate cost-to-go among all S_{t+1} in the set [20]. The mathematical expression is

$$S_{t+1} = \text{argmin}_{S \in N(S_t)} J(S) \quad (19)$$

where S_t is the state at Stage *t*. $N(S_t)$ is the set of all possible states at Stage $t+1$. $J(S)$ is the approximate cost-to-go $\tilde{J}_{t+1}$ of the better one of the two heuristics, expressed as the function of state S. The rollout control u_{it} for all ASEVs *i* is the control that corresponds to the transition from S_t to S_{t+1}.

An alternative expression with the same meaning is given by

$$u_t = \text{argmin}_{u_t \in U_t \text{ and } S \in N(S_t)} [g_t + J(S)] \quad (20)$$

where u_t is the set of control decisions for all ASEVs *i* at Stage *t*, i.e. $u_t = \{u_{it} \text{ for all } i\}$. U_t is the constraint set for u_t at Stage *t*. S_t, $N(S_t)$, and $J(S)$ is defined in (19). g_t is defined in (6).

This process iterates until S_t, S_{it}, and u_{it} for all stages *t* are determined. The sequence of u_{it} for all ASEVs *i* and all stages *t* constitute an optimal control strategy, which controls each ASEV to charge, idle, and work at each stage.

IV. SIMULATION RESULTS

In this chapter, case studies are performed to validate the ASEV dynamics model and the customized rollout approach. The case studies are based on Bristol Airport, a medium-sized airport in the UK. Considering the scale of the airport, the number of ASEVs is set as 35. The renewable power output profiles are obtained from [24]. The battery charging type is at a constant power of 22 kW [25]. The battery cycle efficiency is 90% [26]. To prevent overcharge and deep discharge, the upper and lower threshold of SoC of each battery is 20% and 80%. If the SoC of the battery is over 80% or lower than 20%, the degradation cost will increase significantly. The battery capacity is collected from the existing reference [27]. The case studies consider photovoltaic (PV) generation. The price for PV energy is £0.04/kWh. This model was built via YALMIP in MATLAB R2021a and solved by Cplex on a laptop with Intel Core i7 CPU 3.2-GHz and 32GB RAM.

A. Scenario 1): Comparison between the 'greedy charging' and the rollout algorithm for a typical sunny month in summer

One typical month in summer is chosen for the case study. The workload of serving any given flight is a random variable.

The random workload model is explained in Section III-A. Each flight is served by one ASEV.

The SoC of the ASEVs under the 'greedy charging' algorithm is shown in Fig. 3 Compared with the control algorithm, the 'greedy charging' algorithm is set as the benchmark. The SoC of the ASEVs under the 'rollout approach' strategy is shown in Fig. 4. Each colour in the two figures represents an ASEV.

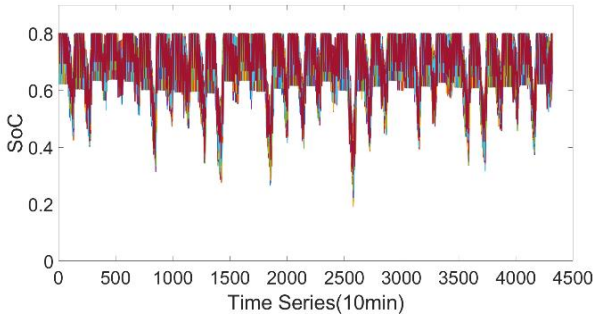

Figure 3. The SoC of the ASEVs in the summer month under rollout algorithm.

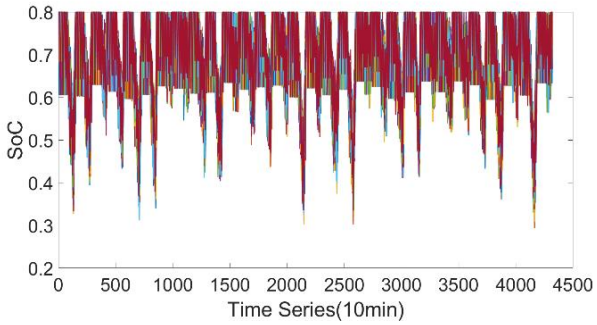

Figure 4. The SoC of the ASEVs in the summer month under 'greedy charging' algorithm.

The operation costs of ASEVs under the two different algorithms are shown in Fig. 5.

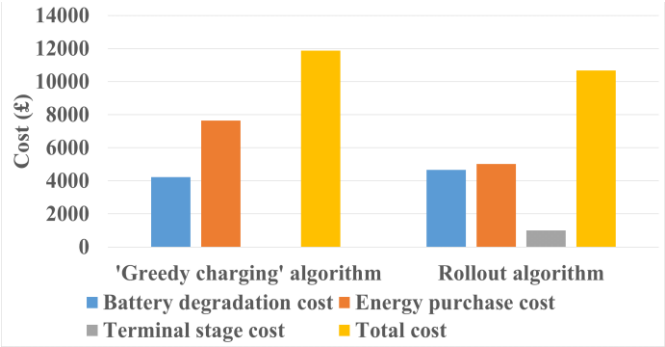

Figure 5. The cost of Bristol Airport under 'greedy charging' and rollout algorithm in the summer month.

When the 'greedy charging' algorithm is applied, in the summer month, for every time slot, there is no ASEV working beyond the upper bound or under the lower bound of its SoC range. It is assumed that there is no punishment for the ASEV's late departure. The total cost is £11,871.3 for the airport in the month. The battery degradation cost, energy purchase cost and terminal stage cost are about £4,221.3, £7,649.7 and £0 respectively.

If the rollout algorithm is applied, the total cost in the summer month is £10,673.2 for the airport. This is broken down into the battery degradation cost, energy purchase cost, and terminal stage cost of £4,668.6, £5,012.1, and £922.4, respectively.

From the comparison of the 'greedy charging' algorithm and the rollout algorithm, it is clear that the rollout algorithm incurs a total cost of 10.5% less than that of the 'greedy charging' algorithm. The battery degradation cost and energy purchase cost of the rollout algorithm is 11.1% more than and 51.3% less than those of the 'greedy charging' algorithm, respectively. In Fig. 4, it is shown that using the rollout algorithm, the ASEV battery may have an SoC below the lower bound. This is because the ASEV would be charged without considering possible flight delays. However, the rollout algorithm achieves a significant saving in the energy purchase cost, compared to the 'greedy charging' algorithm, because: the 'greedy charging' algorithm does not care about the electricity price at all but charges the battery whenever the SoC is not at the maximum. In contrast, the rollout algorithm takes advantage of both the cheap PV energy and the low tariff period of the grid-supplied energy.

In Fig. 3 and Fig. 4, the charging-discharging frequency of 'greedy charging' is greater than that of the rollout algorithm. However, the battery degradation cost under the 'greedy charging' algorithm is less than that under the rollout algorithm. This is because under the 'greedy charging' according to Heuristic ii), the average SoC at the start of charging is greater than that under the rollout algorithm. In other words, the rollout algorithm leads to deeper discharges and thus a greater battery degradation cost than the 'greedy charging' algorithm. Secondly, as mentioned above, occasionally, the SoC of the ASEV under the rollout algorithm drops below the lower threshold, resulting in a higher-than-usual degradation cost. The terminal stage cost of 'greedy charging' is £0 because it charges an ASEV battery whenever it is not full and the ASEV is not working, regardless of the electricity price. This ensures that the ASEV batteries all have the maximum SoC value at the end of the day, resulting in a zero terminal stage cost. In contrast, the rollout algorithm only charges the ASEV batteries when the electricity price is low. As a result, at the end of the day, not all ASEV batteries are fully charged, causing a positive terminal stage cost.

From the simulation results, considering the total cost, the rollout algorithm may be better than the 'greedy charging' algorithm. But in future, if the degradation cost increases, the 'greedy charging' algorithm can be set as a possible protection control strategy for the ASEVs.

V. CONCLUSIONS

This paper proposes a new dynamics model for airport service electric vehicles (ASEVs) and a new customized rollout approach as an optimal control method for the ASEV dynamics model. Case studies compare the rollout algorithm and the 'greedy charging' algorithm (it charges the battery whenever its SoC is not the maximum) for a typical summer month. The summer month has very different PV output profiles and tariffs. In the case study, the 'rollout algorithm' achieves a lower total cost than the 'greedy charging' algorithm. This is because the rollout algorithm takes advantage of the cheap PV energy as well as the off-peak price of the grid-supplied energy, with lower energy cost and total cost. However, the 'greedy charging' algorithm can help reduce the degradation cost. The battery of the ASEV under the 'greedy charging' algorithm may work for a longer time than the rollout algorithm. The research outcome will guide the airport to control the ASEV based on the transportation electrification in the airport. Future work will focus on an improvement of base algorithms for the rollout approach and applying the rollout approach to a larger airport with a more complex situation.

REFERENCES

[1] "Electric Vehicles," House of Parliament, 2010, Available: http://researchbriefings.files.parliament.uk/documents/POST-PN-365/POST-PN-365.pdf.

[2] D. Wu, H. Zeng, C. Lu, and B. Boulet, "Two-Stage Energy Management for Office Buildings With Workplace EV Charging and Renewable Energy," *IEEE Transactions on Transportation Electrification*, vol. 3, no. 1, pp. 225-237, 2017.

[3] Z. Liu, Q. Wu, M. Shahidehpour, C. Li, S. Huang, and W. Wei, "Transactive Real-time Electric Vehicle Charging Management for Commercial Buildings with PV On-site Generation," *IEEE Transactions on Smart Grid*, pp. 1-1, 2018.

[4] C. Lin, D. Deng, C. Kuo, and Y. Liang, "Optimal Charging Control of Energy Storage and Electric Vehicle of an Individual in the Internet of Energy With Energy Trading," *IEEE Transactions on Industrial Informatics*, vol. 14, no. 6, pp. 2570-2578, 2018.

[5] A. Ito, A. Kawashima, T. Suzuki, S. Inagaki, T. Yamaguchi, and Z. Zhou, "Model Predictive Charging Control of In-Vehicle Batteries for Home Energy Management Based on Vehicle State Prediction," *IEEE Transactions on Control Systems Technology*, vol. 26, no. 1, pp. 51-64, 2018.

[6] X. Wu, X. Hu, X. Yin, and S. J. Moura, "Stochastic Optimal Energy Management of Smart Home With PEV Energy Storage," *IEEE Transactions on Smart Grid*, vol. 9, no. 3, pp. 2065-2075, 2018.

[7] M. Rastegar, M. Fotuhi-Firuzabad, H. Zareipour, and M. Moeini-Aghtaieh, "A Probabilistic Energy Management Scheme for Renewable-Based Residential Energy Hubs," *IEEE Transactions on Smart Grid*, vol. 8, no. 5, pp. 2217-2227, 2017.

[8] N. Rahbari-Asr and M. Chow, "Cooperative Distributed Demand Management for Community Charging of PHEV/PEVs Based on KKT Conditions and Consensus Networks," *IEEE Transactions on Industrial Informatics*, vol. 10, no. 3, pp. 1907-1916, 2014.

[9] M. Shafie-khah et al., "Optimal Behavior of Electric Vehicle Parking Lots as Demand Response Aggregation Agents," *IEEE Transactions on Smart Grid*, vol. 7, no. 6, pp. 2654-2665, 2016.

[10] L. Zhang and Y. Li, "Optimal Management for Parking-Lot Electric Vehicle Charging by Two-Stage Approximate Dynamic Programming," *IEEE Transactions on Smart Grid*, vol. 8, no. 4, pp. 1722-1730, 2017.

[11] M. Maigha and M. L. Crow, "A Transactive Operating Model for Smart Airport Parking Lots," *IEEE Power and Energy Technology Systems Journal*, vol. 5, no. 4, pp. 157-166, 2018.

[12] M. Muratori et al., "Technology solutions to mitigate electricity cost for electric vehicle DC fast charging," *Applied Energy*, vol. 242, pp. 415-423, 2019/05/15/ 2019.

[13] K. Seddig, P. Jochem, and W. Fichtner, "Two-stage stochastic optimization for cost-minimal charging of electric vehicles at public charging stations with photovoltaics," *Applied Energy*, vol. 242, pp. 769-781, 2019/05/15/ 2019.

[14] S.-K. Moon and J.-O. Kim, "Balanced charging strategies for electric vehicles on power systems," *Applied Energy*, vol. 189, pp. 44-54, 2017/03/01/ 2017.

[15] M. Weiszer, J. Chen, and G. Locatelli, "An integrated optimisation approach to airport ground operations to foster sustainability in the aviation sector," *Applied Energy*, vol. 157, pp. 567-582, 2015/11/01/ 2015.

[16] X. Li, O. Omotere, L. Qian, and E. R. Dougherty, "Review of stochastic hybrid systems with applications in biological systems modeling and analysis," *EURASIP journal on bioinformatics & systems biology*, vol. 2017, no. 1, pp. 8-8, 2017.

[17] (2016). Bradshaw Electric Vehicles. Available: https://www.airport-suppliers.com/supplier/bradshaw-electric-vehicles/

[18] (2016). Smith Electric Vehicles. Available: https://www.airport-technology.com/contractors/groundequipment/smith-electric/

[19] (2017). Alke Electric Vehicles. Available: https://www.alke.com/doc/alke-atx-electric-vehicles-catalog-eng.pdf

[20] D. P. Bertsekas, Dynamic Programming and Optimal Control, 4th ed. *Athena Scientific*, 2017.

[21] R. S. Sutton and A. G. Barto, Reinforcement learning: an introduction, 2nd ed. *The MIT Press*, 2017.

[22] J. Burkardt, "The Truncated Normal Distribution," Florida State University, 2014, Available: https://people.sc.fsu.edu/~jburkardt/presentations/truncated_normal.pdf.

[23] C. Bordin, H. O. Anuta, A. Crossland, I. L. Gutierrez, C. J. Dent, and D. Vigo, "A linear programming approach for battery degradation analysis and optimization in offgrid power systems with solar energy integration," *Renewable Energy*, vol. 101, pp. 417-430, 2017/02/01/ 2017.

[24] (2019). Weather & Local Environment. Available: http://www.uq.edu.au/solarenergy/pv-array/weather

[25] (2018). Understanding electric car charging. Available: https://www.spiritenergy.co.uk/kb-ev-understanding-electric-car-charging

[26] X. Zhang, Y. Yuan, L. Hua, Y. Cao, and K. Qian, "On Generation Schedule Tracking of Wind Farms With Battery Energy Storage Systems," *IEEE Transactions on Sustainable Energy*, vol. 8, no. 1, pp. 341-353, 2017.

[27] (2021). Electric car boom in Europe starts this year. Available: https://www.eea.europa.eu/en/analysis/indicators/new-registrations-of-electric-vehicles